Phytopathology Research

RESEARCH

Open Access

Enhancing tomato resistance by exploring early defense events against *Fusarium* wilt disease

Jingtao Li[1†], Chenyang Wang[1†], Limei Yang[1], Fahui Qiu[1], Yue Li[1], Yaning Zheng[1], Sihui Liu[2], Limin Song[1*] and Wenxing Liang[1*]

Abstract

Studying plant early immunity, such as the unique immune mechanisms against pathogens, is an important field of research. Tomato wilt resulting from the infection by *Fusarium oxysporum* f. sp. *lycopersici* (*Fol*) is an important soil-borne vascular disease. In this study, we challenged tomato plants with *Fol* for a time-course RNA sequencing (RNA-seq) analysis. The result indicated that phenylpropanoid and flavonoid pathway genes were significantly enriched during the early invasion stage. Further study revealed that the flavonoids galangin and quercetin could effectively inhibit *Fol* growth and enhance wilt resistance in tomato. Moreover, the genes involved in plant-pathogen interactions, the MAPK signaling pathway, and plant hormone signal transduction were significantly enriched. These genes were also involved in plant pattern-triggered immunity (PTI) and effector-triggered immunity (ETI) signaling pathways. Strikingly, the transcription levels of pathogen-related protein 1 (*SlPR1*) were dramatically increased at 2 days post *Fol* inoculation, implying that *SlPR1* is important in early immunity in tomato. SlPR1 does not have direct antifungal activity. Instead, its C-terminal peptide CAPE1 could activate root defense responses, such as the reactive oxygen species (ROS) burst, salicylic acid (SA)/jasmonic acid (JA) production, and defense-related gene expression, which collectively increased tomato resistance to *Fol* infection. In addition, CAPE1 could induce systemic acquired resistance (SAR). Application of CAPE1 onto tomato leaves induced local resistance to the pathogen *Botrytis cinerea* and systemic resistance to *Fol* infection. These results advanced our understanding for the early immunity against *Fol* in tomato and provide potential strategy for tomato disease control.

Keywords Plant immunity, *SlPR1*, CAPE1, Induced systemic resistance, Tomato

Background

Plants are naturally challenged by various harmful microorganisms and parasites. Owing to their preformed defenses and innate immune system, plants are capable of defeating most potential microbial invaders (Zhang et al. 2017; Cao et al. 2018). A large number of pattern recognition receptors (PRRs) in plant cell surface can recognize conservative pathogen-/damage-/microbe-associated molecular patterns (PAMPs/DAMPs/MAMPs) to activate PAMP-triggered immunity (PTI) (Zipfel 2008). In addition, plants have also evolved intracellular nucleotide-binding leucine-rich repeat receptors (NLRs) to

†Jingtao Li and Chenyang Wang contributed equally to this work.

*Correspondence:
Limin Song
liminsong@qau.edu.cn
Wenxing Liang
wliang1@qau.edu.cn
[1] College of Plant Health and Medicine, Engineering Research Center for Precision Pest Management for Fruits and Vegetables of Qingdao, Shandong Engineering Research Center for Environment-Friendly Agricultural Pest Management, Shandong Province Key Laboratory of Applied Mycology, Qingdao Agricultural University, Qingdao 266109, China
[2] College of Science and Information, Qingdao Agricultural University, Qingdao 266109, China

recognize effectors and initiate effector-triggered immunity (ETI) (Dangl et al. 2013). Though PTI and ETI are activated by different mechanisms and involve different signaling cascades, recent reports show that activation of PRRs and NLRs ('PTI + ETI') leads to the coactivation of multiple immunity-related components, such as calcium channels, CPKs, MAPKs, and NADPH oxidases (Yuan et al. 2021; Ngou et al. 2022). This results in a calcium influx, reactive oxygen species (ROS) burst, and transcriptional reprogramming, which further leads to the accumulation of pathogenesis-related proteins (PRs), production of defense-related phytohormones and biosynthesis of antimicrobial compounds. As a result, it restricts pathogen infection (Ngou et al. 2022).

During pathogen infection, PR1 is one of the abundantly produced plant PR proteins, and its expression has been used as a marker for salicylic acid (SA)-activated systemic acquired resistance (SAR) (Breen et al. 2017). Although PR1 proteins have been studied for several decades as a resistance protein, its biochemical function in plant immunity remains largely elusive (Breen et al. 2017; Kong et al. 2020). PR1 not only has a direct anti-oomycete activity through its binding to pathogen sterols but also produces a conserved defense signaling peptide CAPE1 at its C-terminus, in response to wounding or methyl jasmonate treatment (Woloshuk et al. 1991; Niderman et al. 1995; Choudhary and Schneiter 2012; Chen et al. 2014; Gamir et al. 2016; Breen et al. 2017; Sung et al. 2021). A recent study showed that the fungal effector SnTox3 from *Parastagonospora nodorum* could target TaCAPE1 of wheat TaPR1 to suppress host defense by preventing it release (Sung et al. 2021). We recently reported that the *Fusarium oxysporum* secreted effector FolSvp1 enhanced virulence by translocating the tomato SlPR1 to nucleus to impede CAPE1 release (Li et al. 2022). These results indicated that apoplastic PR1 and its C-terminal peptide are integral components in the defense of tomato plants, which makes PR1 be a strong selective pressure for pathogens to bypass (Breen et al. 2017).

Plants produce a wide variety of secondary metabolites, and many of which have selective advantages against microbial attacks (Dixon 2001; Tugizimana et al. 2019). During the plant immune activation, the levels of the secondary metabolites phenylpropanoids and flavonoids, which are also known as phytoalexins, are largely increased. Flavonoid biosynthesis is an essential branch of phenylalanine metabolism, and the production of these compounds is facilitated by PTI (Zaynab et al. 2018; Sharma et al. 2020; Liu et al. 2023). Previous studies have revealed that flavonoids (e.g., flavonols, isoflavones, and flavanones) directly suppress conidial germination and hyphal growth of fungal pathogens (Long et al. 2019). For instance, a yellow lupine isoflavone, genistein, can strongly reduce several diseases caused by the phytopathogenic fungi *Aspergillus flavus*, *F. oxysporum*, and *Sclerotinia sclerotiorum* (Morkunas et al. 2005). Similarly, tannins are effective chemical agents to defend against *Melampsora larici-populina*, which causes rust diseases on plants (Ullah et al. 2017). The rice flavanone sakuranetin exhibits dramatic inhibitory activity on the pathogens *Pyricularia oryzae* and *Rhizoctonia solani* (Katsumata et al. 2018). These findings indicated that secondary metabolites can potentially combat plant pathogens; however, there are still many defence-related metabolites that need to be explored.

Tomato (*Solanum lycopersicum*) is a popular vegetable species worldwide. *F. oxysporum* is a soil-borne fungal pathogen that causes *Fusarium* wilt disease in a vast array of plant species (Michielse and Rep 2009). Specifically, *F. oxysporum* f. sp. *lycopersici* (*Fol*), the causal agent of tomato *Fusarium* wilt disease, infects tomato roots and colonizes xylem vascular tissue, thereby blocking water transport and causing wilting and substantial loss of yield (Michielse and Rep 2009; Yin et al. 2021). Plant early immunity is an important focus of research and understanding of plant early immunity can provide valuable information for the application of plant immune mechanisms to defend against pathogens. The omics and bioinformatics can greatly increase our understanding in the regulation of plant defense mechanisms against pathogens (Li et al. 2021). However, the global transcriptional reprogramming of tomato immunity during the early response to *Fol* remains largely unclear. In this study, we highlighted the early immune events of tomato against *Fol* at the transcriptomic level and explored key metabolites and resistance proteins for controlling tomato *Fusarium* wilt. The resulting identified flavonoids (galangin and quercetin) and the resistance peptide CAPE1 of tomato PR1 potentially combat plant pathogens, and these compounds used for disease management are safe for both humans and the ecosystem.

Results

Early infection with *Fol* induced tomato transcriptome reprogramming

To identify early immune events in tomato in response to *Fol* infection, we performed time-series inoculation experiments (Fig. 1a). By surveying the relative *Fol* biomass via quantitative polymerase chain reaction (qPCR), we found that *Fol* was present in host roots as early as 2 days post-inoculation (dpi), indicating an early invasive colonization of *Fol* (Fig. 1b). To explore the transcriptional reprograming of tomato host plants in response to this early infection by *Fol*, genome-wide time-series RNA sequencing (RNA-seq) data from root tissue harvested at 0, 1, 2, and 3 dpi were analyzed (Fig. 1a). In total, 12

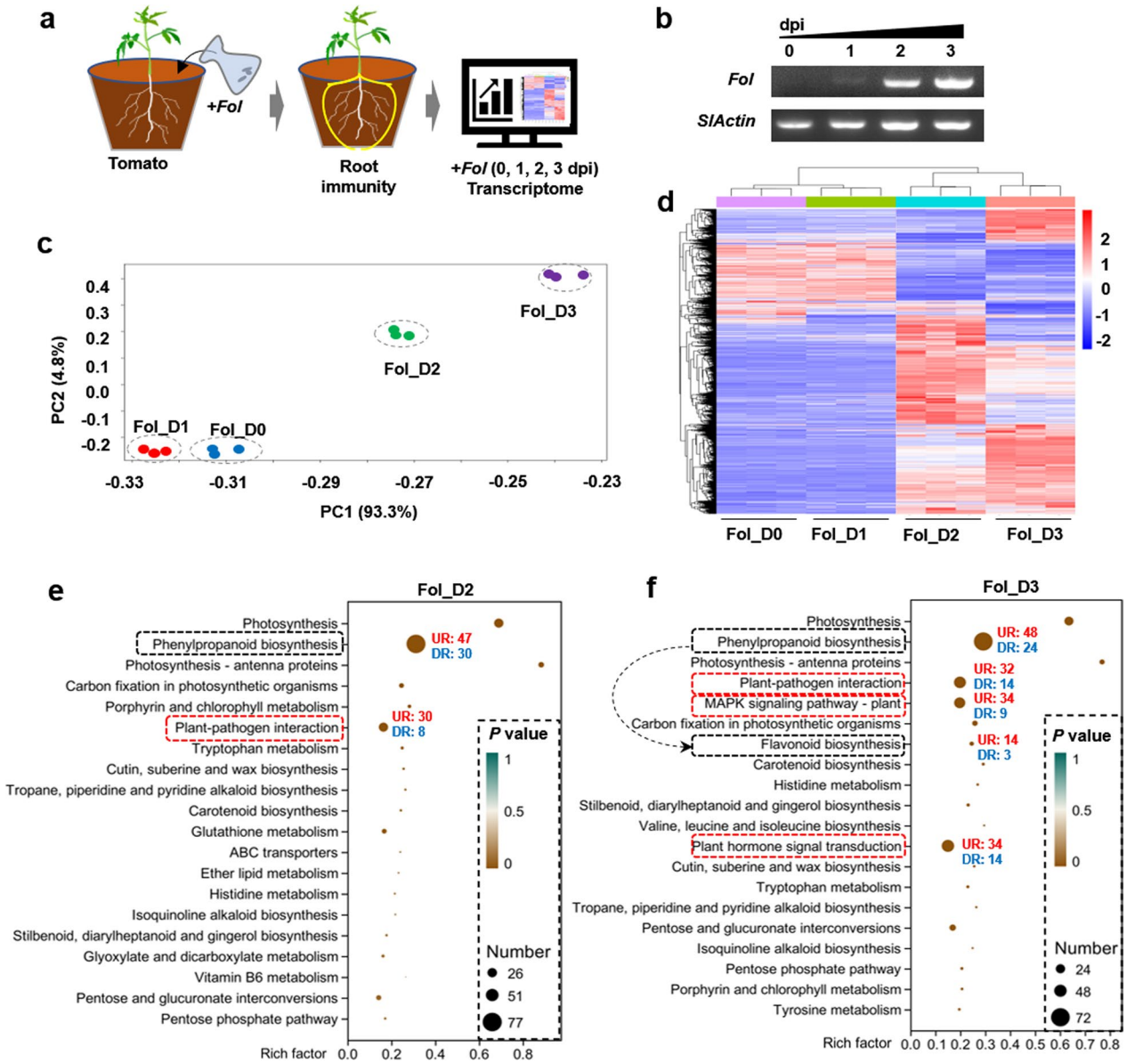

Fig. 1 Tomato root early responses to *Fol* infection at the transcriptomic level. **a** Schematic diagram illustrating the process of obtaining transcriptomic data at different time points (Fol_D0, Fol_D1, Fol_D2, and Fol_D3) after *Fol* inoculation. **b** Biomass of *Fol* in host roots during the early invasion stage. Total DNA was isolated from tomato roots inoculated with *Fol* at the indicated times, and PCR was performed. **c** PCA results of the transcriptomic data. **d** Heatmap showing the hierarchical clustering of DEGs upon expression of Fol_D0, Fol_D1, Fol_D2, and Fol_D3 in tomato roots. The color scale indicates the Z score. The full lists can be found in Additional file 1: Table S1. **e**, **f** KEGG pathway-based enrichment analysis of the significant DEGs detected at 2 days (**e**) and 3 days (**f**) after *Fol* inoculation relative to those of tomato roots prior to *Fol* inoculation (Fol_D0)

samples (4 time points with each 3 biological replicates) were harvested for library construction. After filtering out low-quality ends of reads and trimming adaptor sequences, we mapped approximately 37.2 to 46.8 million clean reads from different samples to the *S. lycopersicum* reference genome (Additional file 1: Table S1).

To investigate the global differences in the transcriptome dynamics during *Fol* infection, we performed principal component analysis (PCA) (Fig. 1c). The results showed a high similarity among the biological replicates. The two early stages after *Fol* inoculation (Fol_D0 and Fol_D1) showed the strongest correlation, indicating that their transcriptional programs were highly similar. After 2 dpi, the root transcriptome responses (Fol_D2 and Fol_D3) showed substantial differences (Fig. 1c). These findings indicated that *Fol* infection might induce substantial

transcriptome reprogramming in tomato roots and the host defense begins at 2 dpi.

To identify the genes whose expression levels are higher in response to *Fol* infection, we considered genes that the absolute value of the expression fold-change (FC) was ≥ 2 and the false discovery rate (FDR) was ≤ 0.05 in any two time points. Overall, 5219 differentially expressed genes (DEGs) were obtained (Additional file 2: Figure S1a, b). Compared to those in uninfected tomato (Fol_D0), the number of upregulated genes at 1 dpi (Fol_D1) increased from 96 to 1835 at 2 dpi (Fol_D2) and to 1887 genes at 3 dpi (Fol_D3), whereas the number of downregulated genes increased from 216 at 1 dpi to 531 at 2 dpi and then increased to 652 genes at 3 dpi (Additional file 2: Figure S1a). Among them, 1388 DEGs were the same at 2 dpi and 3 dpi (Additional file 2: Figure S1b), indicating that there were cooperatively mediated changes in host gene expression during infection. A heatmap depicting the stage-specific expression of the genes in the roots was constructed and is shown in Fig. 1d. Notably, there were more upregulated genes at 2 and 3 dpi than those at 1 dpi, supporting the notion that *Fol* induced host defense gene expression during invasion. Moreover, these data showed that 2–3 dpi could be a critical time point for transcriptome reprogramming to defend against early pathogen infection.

Kyoto Encyclopedia of Genes and Genomes (KEGG) pathway analysis of DEGs revealed the main host defense events

To explore the biological functions contributing the most to early infection defense in the roots, we performed KEGG analyses using the DEGs at 2–3 dpi. Our results showed that the genes that were differentially expressed at 2 dpi were enriched in 105 pathways, whereas the genes that were differentially expressed at 3 dpi were enriched in 103 pathways (Additional file 1: Table S2). The most significantly enriched KEGG pathways at 2 dpi were those related to photosynthesis, photosynthesis-antenna proteins, phenylpropanoid biosynthesis, and plant-pathogen interactions (Fig. 1e). At 3 dpi, three additional pathways, the flavonoid biosynthesis, MAPK signaling, and plant hormone signal transduction, were markedly enriched, with each pathway up to 77 genes (Fig. 1f and Additional file 1: Table S2).

Based on their biological processes, these DEG-enriched pathways could be classified into three classes. Class I contains 136 DEGs involved in plant-pathogen interactions, MAPK signaling, and plant hormone signal transduction (Additional file 1: Tables S2, S3). Among these DEGs, eight genes are involved in the three pathways, highlighting their multiple layers of importance in defense regulation (Additional file 2: Figure S2a). Moreover, more DEGs in this class were upregulated than downregulated at 2 and 3 dpi (Additional file 2: Figure S2a), which further supported the notion that they are involved in the activation of plant immune defense. The class II DEGs are involved in photosynthesis. This class includes two categories of KEGG pathway terms, the photosynthesis and photosynthesis-antenna proteins (Additional file 1: Table S2). In response to *Fol* infection, 59 upregulated genes involved in photosynthesis and photosynthesis-antenna proteins were detected at 2 dpi (Fig. 1e), and 54 genes were upregulated at 3 dpi (Fig. 1e). However, few genes were downregulated at 2 and 3 dpi (Fig. 1e, f). These findings indicated that photosynthesis pathway was significantly activated. Class III DEGs are involved in secondary metabolism. These DEGs are enriched in the phenylpropanoid and flavonoid biosynthesis pathways. In this class, 47 genes were upregulated at 2 dpi, and 48 genes were upregulated at 3 dpi (Fig. 1e, f and Additional file 1: Table S2). There were 30 and 24 downregulated genes at 2 and 3 dpi, respectively. The overlapping of 14 DEGs indicated that the two metabolic pathways are closely related (Additional file 2: Figure S2b). The abundance of genes upregulated at 2 and 3 dpi indicated that substantial changes in secondary metabolism took place in tomato roots, and some of which could be related to the production of antimicrobial compounds. Overall, by increasing the expression of the genes involved in the immune signaling pathway, photosynthesis, and secondary metabolism in roots, *Fol* infection activated the defense in tomato plants.

Activation of the PTI and ETI signaling pathways in response to *Fol* infection

Plants respond to pathogens generally by the use of a two-tier innate immune pathway activated by either cell-surface PRRs or intracellular NLR receptors, resulting in PTI or ETI (Ngou et al. 2022). Upon *Fol* infection on the tomato plants, most markedly enriched DEGs in class I were involved in multiple PTI and ETI immune signaling pathways (Fig. 2a and Additional file 1: Tables S2, S3). Some DEGs were involved in phosphorylation and processes involving transcription factors (TFs) and hormones. The roles in defense regulation of a small number of DEGs were unclear, and we marked them as 'others'.

In PTI activation, PRRs are usually associated with either the plasma membrane receptor-like kinases (RLKs) or receptor-like proteins (RLPs), where they perceive P/M/DAMPs to activate the PTI signaling pathway (Ngou et al. 2022). Here, twelve PRR genes, ten encoding LRR-RLKs, and two encoding LRR-RLPs, were upregulated upon *Fol* infection; whereas four LRR-RLK genes were downregulated (Fig. 2a). The somatic embryogenesis receptor kinase 2-like (SERK2)

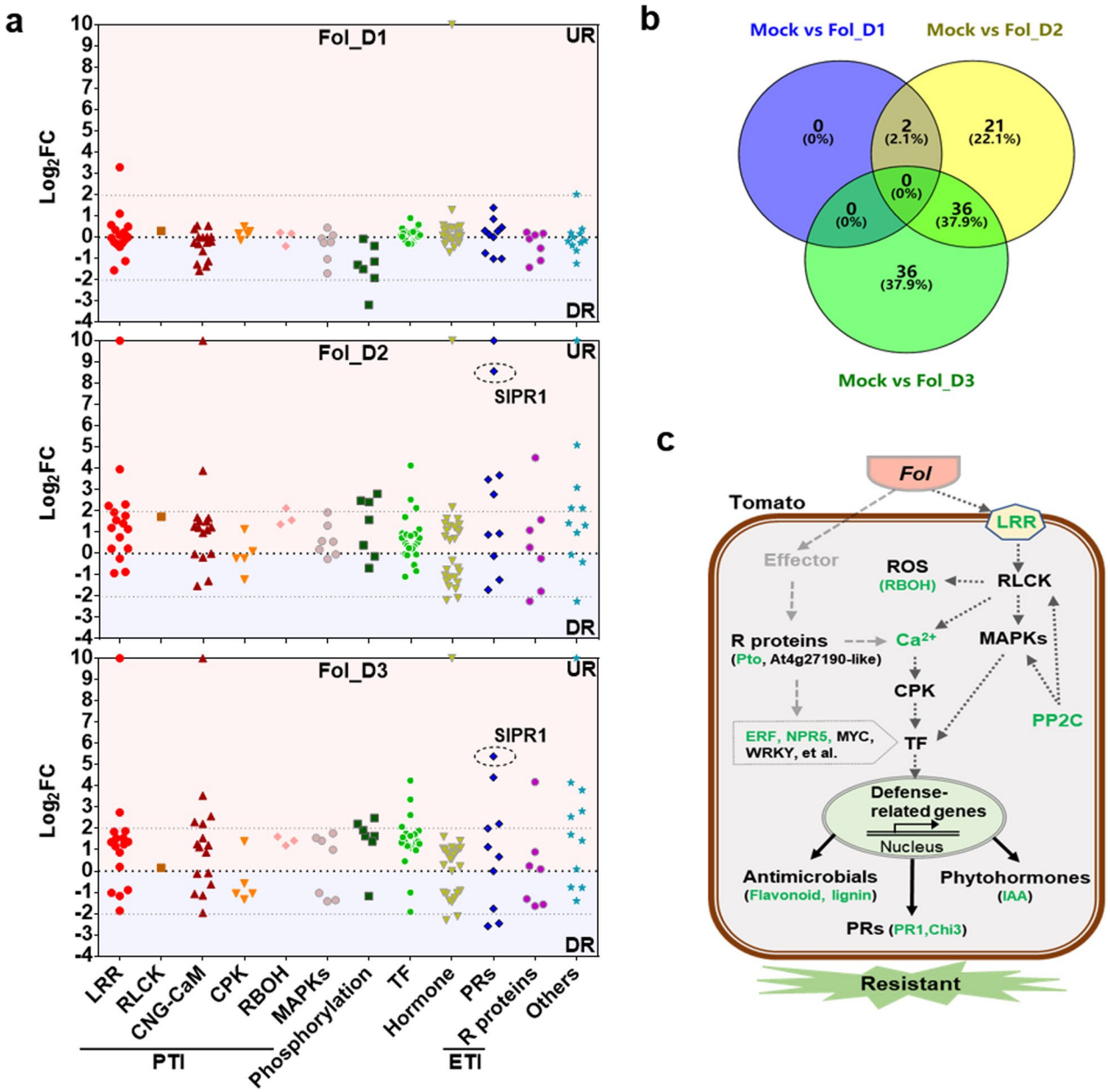

Fig. 2 Expression patterns of the significant DEGs involved in plant immune signaling pathways. **a** Expression patterns of DEGs involved in PTI, ETI and other immunity responses. These DEGs are involved in plant-pathogen interactions, MAPK signaling, and plant hormone signal transduction based on the results of the KEGG pathway analysis. UR, upregulated. DR, downregulated. **b** Venn diagram showing the upregulated DEGs from **a**. **c** Pathway showing the signaling components encoded by DEGs upregulated during early *Fol* infection. The DEGs for the $\log_2$(FC) > 2 are highlighted in green

was predicted as a putative RLCK that is not well characterized in tomato immunity. This RLCK gene was at the downstream of PRRs and was also upregulated at 2 dpi, but its expression subsequently was decreased to the normal levels at 3 dpi. Calcium is an important signaling molecule in response to stress. There were twelve upregulated and four downregulated DEGs encoding cyclic nucleotide-gated (CNG) ion channel proteins or calmodulin (CaM) Ca^{2+}-binding proteins, which are likely related to calcium influx. In addition, there were one upregulated and four downregulated DEGs encoding calcium-dependent protein kinases (CPKs). Moreover, four upregulated and three downregulated DEGs were involved in the

mitogen-activated protein kinase (MAPK) signaling pathway. As expected, three respiratory burst oxidase homolog protein (RBOH) genes were obviously upregulated, which might contribute to ROS accumulation. These transcriptional changes in PTI signaling components strongly indicated that PTI was activated during *Fol* infection. In ETI, there were three upregulated and four downregulated DEGs encoding plant disease resistance (*R*) proteins that may perceive pathogen effectors (Fig. 2a). Although the number of upregulated genes involved in ETI was much lower than that in PTI, the transcriptional response still suggested that ETI was also activated.

Moreover, there were seventeen upregulated genes and only one downregulated gene encoding TFs, indicating that multiple defense-related TFs increased in abundance with PTI and ETI activation. Among them, WRKY, MYC1/2, ethylene responsive element binding protein (ERB), and ethylene-responsive factor (ERF) TFs are related to defense-related hormones, such as ethylene (ET), jasmonic acid (JA), and SA. In addition, there were fourteen upregulated and thirteen downregulated DEGs related to indoleacetic acid (IAA), abscisic acid (ABA), brassinosteroids (BRs), and gibberellic acid (GA). These findings suggested that hormones were also affected upon *Fol* early infection. PR protein expression is generally used to monitor the plant defense response during pathogen invasion. Among the DEGs encoding PR proteins assigned to class I, there were seven upregulated and three downregulated genes. Among the upregulated genes, four genes encode PR1 family proteins. Moreover, there were two upregulated genes that encode endochitinase, which belong to PR3 family. These proteins could act to degrade fungi cell wall and inhibit conidia germination (Zhang et al. 2020). Together, these findings showed that substantial changes took place in PTI pathways and several ETI signaling pathways. Notably, 69.9% (95/136) of the genes were upregulated (Fig. 2a and Additional file 1: Table S3). Among the upregulated DEGs (Fig. 2b), 21 were upregulated only at 2 dpi, and 36 genes were upregulated only at 3 dpi. There were 36 genes whose expression patterns were the same between 2 and 3 dpi, which indicated that sustained expression might be required in response to *Fol* infection. These upregulated genes were widely involved in multiple components of the PTI and ETI signaling pathways (Fig. 2c and Additional file 1: Table S3). Specifically, 31 genes were markedly upregulated in accordance with a $\log_2$(fold-change [FC]) greater than 2 (Fig. 2c and Additional file 1: Table S4). These results further highlighted that PTI- and ETI-mediated basal immunity was strongly activated during *Fol* infection.

Activation of flavonoid metabolism contributes to tomato resistance to *Fol*

PTI-induced transcriptional regulation results in the biosynthesis of antimicrobial compounds (Ngou et al. 2022). The biosynthesis pathway of phenylpropanoid starts from phenylalanine, which can be converted into aromatic compounds including benzenoids, flavonoids, hydroxycinnamates, coumarins, and lignin (Geng et al. 2020). Currently, several enzymes involved in the phenylpropanoid and flavonoid biosynthesis pathways have been identified, including lyases, transferases, ligases, oxygenases, and reductases (Geng et al. 2020). Upon early stage of *Fol* infection, a total of 63 significantly upregulated genes encoding seven types of enzymes were identified in the phenylpropanoid and flavonoid pathways (class II) in tomato plants (Additional file 2: Figure S2c, d). Among these genes, two genes were upregulated from 1 to 3 dpi. Thirty-six genes (> 50%) were upregulated at 2 and 3 dpi. In the other cases, 11 genes were upregulated only at 2 dpi, and 13 genes were upregulated at 3 dpi. The upregulation of the genes in this pathway suggested that the accumulation of their respective metabolites might increase in response to *Fol* infection.

To explore the metabolites that have potential antimicrobial properties, we performed a KEGG analysis using the significantly upregulated genes in class II. Due to the similar backbones, the pathways of the metabolites phenylpropanoid and flavonoid are highly interconnected. As shown in Fig. 3a, there are some overlaps as well. Based on the KEGG analysis, ten natural metabolites are potentially related when tomato plants are infected by *Fol*. Among these metabolites, p-hydroxyphenyl lignin, guaiacyl lignin, 5-hydroxyguaiacyl lignin, syringyl lignin, and coniferin are downstream of the phenylpropanoid pathway. The other five products, pinostrobin, galangin, quercetin, myricetin, and homoeriodictyol, are flavonoid products derived from the flavonoid biosynthesis pathway. To test the possible effects of their properties on *Fol* infection, two lignin products (lignine and sodium lignosulfonate), coniferin, and five flavonoids were used for antifungal assays (Fig. 3b, c). By measuring the microbial growth curve, we found that at concentrations of 125 μg/L, galangin, pinostrobin, lignine, and quercetin effectively inhibited the growth of *Fol* (Fig. 3b). However, when their concentration decreased to 62.5 μg/L, only the flavonoids galangin and quercetin stably inhibited the growth of *Fol* (Fig. 3b). Furthermore, the antifungal activity of galangin and quercetin was tested by a plate assay. The results revealed 11.4% and 9.4% inhibition rates, respectively (Fig. 3c). Moreover, pretreatment with galangin and quercetin increased tomato resistance to *Fol* (Fig. 3d). Taken together, these results suggested that galangin and quercetin were toxic to pathogens.

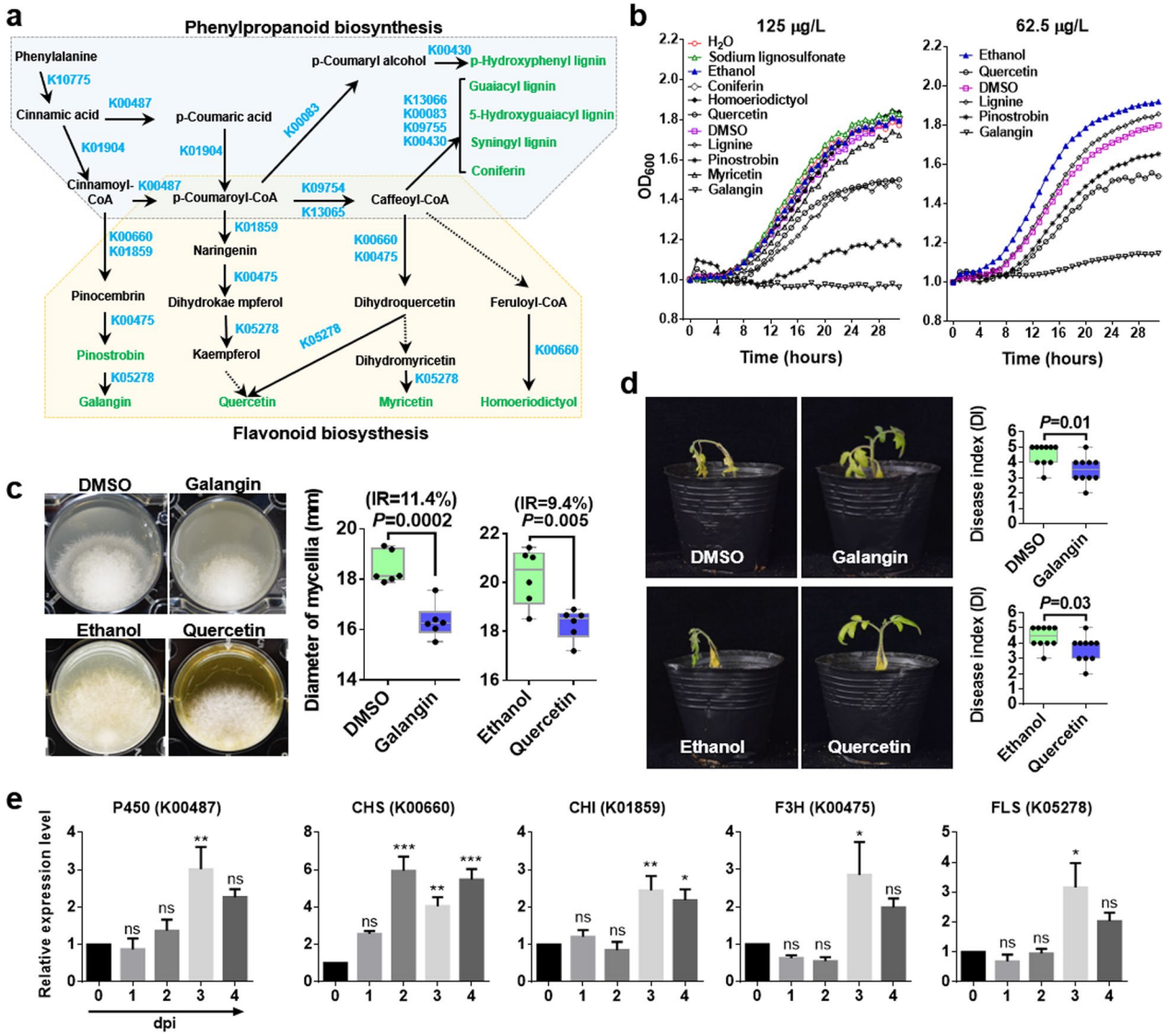

Fig. 3 Flavonoids that contribute to tomato resistance to *Fol*. **a** Simplified phenylpropanoid and flavonoid pathway showing the branches including lignin, coniferin and flavonol metabolite synthesis. The significantly upregulated DEGs were enriched in the biosynthesis pathway based on KEGG analysis. **b** Antimicrobial activity of the synthetic metabolite candidates at concentrations of 125 μg/mL (left) and 62.5 μg/mL (right). The OD_{600} was used to evaluate the antimicrobial activity. **c** Inhibition of *Fol* growth in the presence of galangin or quercetin. Mycelium-colonized agar plugs were cultured for 2 days on PDA media that included 62.5 μg/mL galangin or quercetin at 28°C. The diameter of *Fol* colonies was measured to evaluate growth inhibition. Statistical significance was determined by Student's *t*-test; the *P* values are shown. **d** Resistance of tomato pretreated with galangin or quercetin prior to *Fol* infection. Inoculation assay was carried out 20 min after irrigation with 62.5 g/mL galangin or quercetin. Disease index of 10 plants was scored at 14 dpi. Statistical significance was determined by Student's *t*-test; the *P* values are shown. **e** qRT-PCR validation of galangin- and quercetin-related genes in tomato root against *Fol* infection. The expression levels were normalized to those of *SlActin*. The data represent the means ± SEs of three technical repeats. The experiment was repeated twice with similar results. (Student's *t*-test; ns, no significant difference; $^{*}P < 0.05$; $^{**}P < 0.01$; $^{***}P < 0.001$)

Flavonoid biosynthesis is regulated by the transcription of genes encoding chalcone synthase (CHS), chalcone isomerase (CHI), flavonoid-3-hydroxylase (F3H), and flavonol synthase (FLS) (Sharma et al. 2020). In addition, microsomal cytochrome P450 enzymes, which are flavonoid hydroxylases, are also responsible for the hydroxylation of flavonoids. These proteins are the major enzymes catalyzing the biosynthesis of flavonoids from phenylalanine. In the present study, on the basis of both the transcriptomic data (Additional file 1: Table S5) and the qRT-PCR results, all of the genes encoding the abovementioned proteins were significantly upregulated

in tomato plants upon *Fol* infection (Fig. 3e), which facilitates the accumulation of flavonoids. Overall, the substantial transcriptomic changes associated with secondary metabolism took place in the plants, and both galangin and quercetin biosynthesis could contribute to the resistance of tomato against *Fol* infection.

The defense protein SlPR1 has no antifungal activity

Notably, one defense gene encoding the pathogen-related protein 1, SlPR1, also known as PR1b1/P14a/P4, was the most markedly upregulated gene at 2 and 3 dpi (Fig. 2a, Additional file 2: Figure S3, and Additional file 1: Table S3). To explore the biological function of SlPR1 in response to *Fol* invasion, we further evaluated its transcriptional level via fragments per kilobase of transcript per million mapped reads (FRPKM) analysis. As shown in Fig. 4a, the levels of *SlPR1* transcripts in the roots were quite low (FRPKM < 1) at 0 and 1 dpi; however, *SlPR1* transcripts were significantly increased at 2 dpi (FRPKM > 300) and 3 dpi (FRPKM > 30). These results indicated the importance of SlPR1 in tomato early defense.

Some PR1 proteins are reported to suppress the growth of oomycetes. For example, owing to the ability of PR1s to chelate sterols to form a sterol auxotroph (pathogen membranes), P14c from *S. lycopersicum* and PR1a from *Nicotiana tabacum* show the growth inhibition activity on zoospores from *Phytophthora infestans* (Breen et al. 2017). Sequence alignment revealed that SlPR1 is 55.6% and 53% identical to the sequences of P14c (tomato; GenBank Accession No. NM001247429) and PR1a (tobacco; D90196), respectively (Fig. 4b, Additional file 2: Figure S4). The conserved and established features with respect to these PR1 proteins (Fig. 4b) indicated that the SlPR1

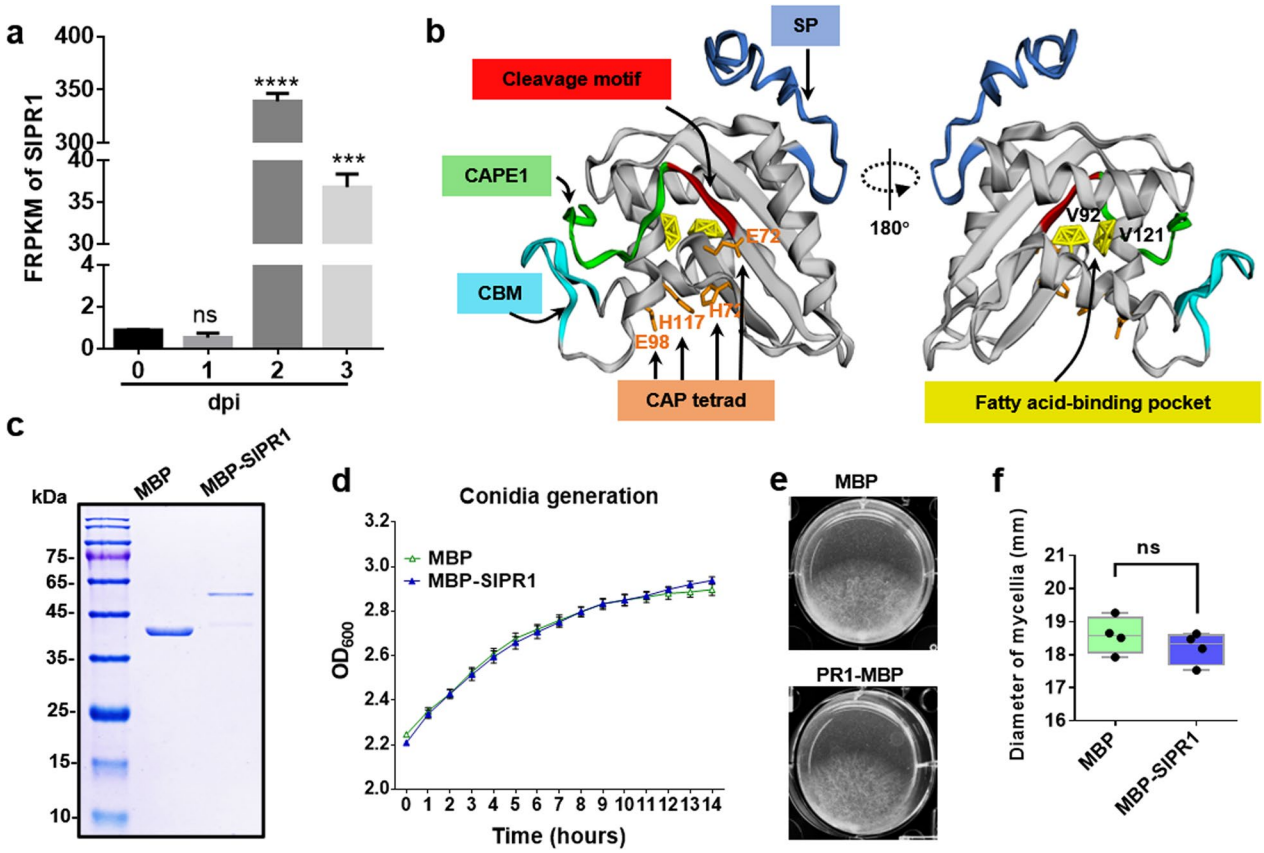

Fig. 4 The defense protein SlPR1 exerts no antifungal activation. **a** Expression profile of *SlPR1* in tomato roots after *Fol* inoculation at the indicated times, as measured by FRPKM data. The data represent the means ± SEs of three independent replicates. (Student's *t*-test; ns, no significant difference; ***$P < 0.001$; ****$P < 0.0001$). **b** Schematic representation of an SlPR1 model based on the predicted protein structure (left and right rotated 180° around the longitudinal axis). The multiple conserved motifs are marked as detailed in Additional file 2: Figure S4. **c** CBB-stained SDS-PAGE gel showing the purity of obtained MBP and MBP-SlPR1. **d** Antimicrobial activity of MBP-SlPR1 recombinant protein. After the addition of 200 μg/mL purified MBP-SlPR1 or MBP to 1×10^6 *Fol* spores/mL to 5% YEPD media, the microtiter plates were incubated on a shaking platform (100 rpm, 25°C). The OD_{600} was used to evaluate the antimicrobial activity. The data represent the means ± SEs (n = 4). **e** Inhibition of *Fol* growth in the presence of 200 μg/mL purified MBP-SlPR1 or MBP proteins. **f** The diameter of *Fol* colonies obtained from the samples in **e**. Statistical significance was revealed by Student's *t*-test. (Ns, no significant difference)

protein might have similar antifungal activity. To this end, MBP-tagged SlPR1 was purified from *Escherichia coli* (Fig. 4c) and incubated with *Fol* conidia. By measuring the microbial growth curve, we found that MBP-SlPR1 displayed no significant inhibitory activity on *Fol* growth (Fig. 4d–f).

The CAPE1 peptide of SlPR1 induces a root-specific defense response and systemic resistance

The endogenous peptide CAPE1, generated by cleavage of the C-terminus of SlPR1 (Fig. 4b), was found to be associated with tomato resistance to *Fol* in our recent study (Li et al. 2022). To further understand the bioactivity of CAPE1 in activating tomato resistance, we determined CAPE1-induced ROS bursts, defense hormone SA/JA production, and defense marker gene expression. Compared with control leaves, tomato roots treated with CAPE1 or flg22 produced a substantial ROS burst (Fig. 5a). In this assay, since the bacterial MAMP flg22 can induce ROS production, it was used as a positive control (Ngou et al. 2022). The result indicated that CAPE1 is likely a self-regulating molecule in activating the root cell responses. However, the SlPR1-MBP protein did not induce ROS production (Fig. 5a), suggesting that CAPE1 release might dominate SlPR1-mediated defenses in tomato. Furthermore, pretreatment with CAPE1 effectively increased H_2O_2 levels (Fig. 5b, c).

The SA and JA signaling pathways are two essential signaling pathways in plant-based resistance. Although the SA/JA pathways are largely antagonistic (Wan and Xin 2022), SA signaling-mediated SAR has also been shown to require JA, which may be an early signal to establish systemic immunity (Vlot et al. 2008; Fu and Dong 2013; Kamle et al. 2020). As shown in Fig. 5d, the defense phytohormones SA/JA, and JA related jasmonate metabolites JA-isoleucine (JA-Ile) and cis-(+)-12-oxo-phytodienoic acid (cis-OPDA) also significantly accumulated in the roots in response to CAPE1 treatment. In addition, both SA- and JA-related genes were significantly upregulated at 2 or 4 hpi in the roots of tomato plants treated with CAPE1 (Fig. 5e). SAR provides long-term resistance to pathogens and is correlated with activation of PR genes, such as *PR1* (unclear function), *PR2* (β-1,3-glucanase), and *PR5* (thaumatin-like protein) (Vlot et al. 2008; Fu and Dong 2013). In the roots of CAPE1-treated plants, *PR1* (*SlPR1*, *P14c*, *PR1a1*), *PR2*, and *PR5* were significantly upregulated (Fig. 5e). Together, these findings suggested that SAR is activated by CAPE1. To further verify this hypothesis, we evaluated the CAPE1-mediated long-distance induction of the hormones SA/JA and defense-related marker genes (Fig. 5d, e). Notably, the SA/JA levels and a few JA/SA-related genes in distant tomato leaves were significantly upregulated. To determine whether this peptide-mediated root defense contributes to tomato resistance to *Fusarium* wilt disease, roots of tomato plants pretreated with or without synthetic CAPE1 were then inoculated with *Fol*. As shown in Fig. 5f and Fig. 5g, only pretreatment with CAPE1 effectively decreased the *Fol* infection, indicating the important role of CAPE1 peptide in tomato defense against *Fol*.

CAPE1 induces the leaf defense response and systemic resistance

Since CAPE1 could activate immune responses in the roots of tomato plants, it was very likely to induce similar defense responses in the plant leaves. As expected, CAPE1 directly induced ROS production and H_2O_2 accumulation in the leaves (Fig. 6a, b). By measuring the SA and JA levels at 4 hpi of CAPE1, we found that the SA, JA, cis-OPDA, and JA-Ile levels significantly increased in the leaves of CAPE1-treated tomato plants compared to the control (Fig. 6c). Similarly, the transcript levels of defense genes involved in the JA and SA signaling pathways were also measured by qRT-PCR (Fig. 6d). Both the SA- and the JA-related genes were significantly upregulated at 2 and 4 hpi in the plant leaves and roots when the leaves were treated with CAPE1. The change of the expression levels for JA-related genes in the tomato roots at 4 hpi was much higher than that of the SA-related genes. Similar to the roots of the CAPE1-treated plants, our data showed that *PR1*, *PR2*, and *PR5* were also significantly upregulated in the leaves of CAPE1-treated plants, suggesting that SAR was activated in the leaves. To directly verify this hypothesis, we pre-sprayed tomato leaves with CAPE1 and performed infection assays with *Fol*. Compared with the control plants, tomato plants whose leaves were treated with CAPE1 showed increased disease resistance to *Fol* (Fig. 6e). The difference in disease severity was confirmed by monitoring the growth with quantitative fresh weight data. The results showed that there was a significant increase in growth of the CAPE1-treated tomato plants upon *Fol* infection (Fig. 6f).

Together, these findings showed that (1) *SlPR1* is upregulated in response to *Fol* infection; (2) purified SlPR1 exerts no antimicrobial activity or ROS activation; and (3) the CAPE1 peptide has bioactivity, including the production of ROS and the subsequent induction of defense-related marker genes. Thus, these findings suggest that there is an important role of SlPR1 in disease resistance in tomato, which is dependent on the SlPR1 C-terminal CAPE1.

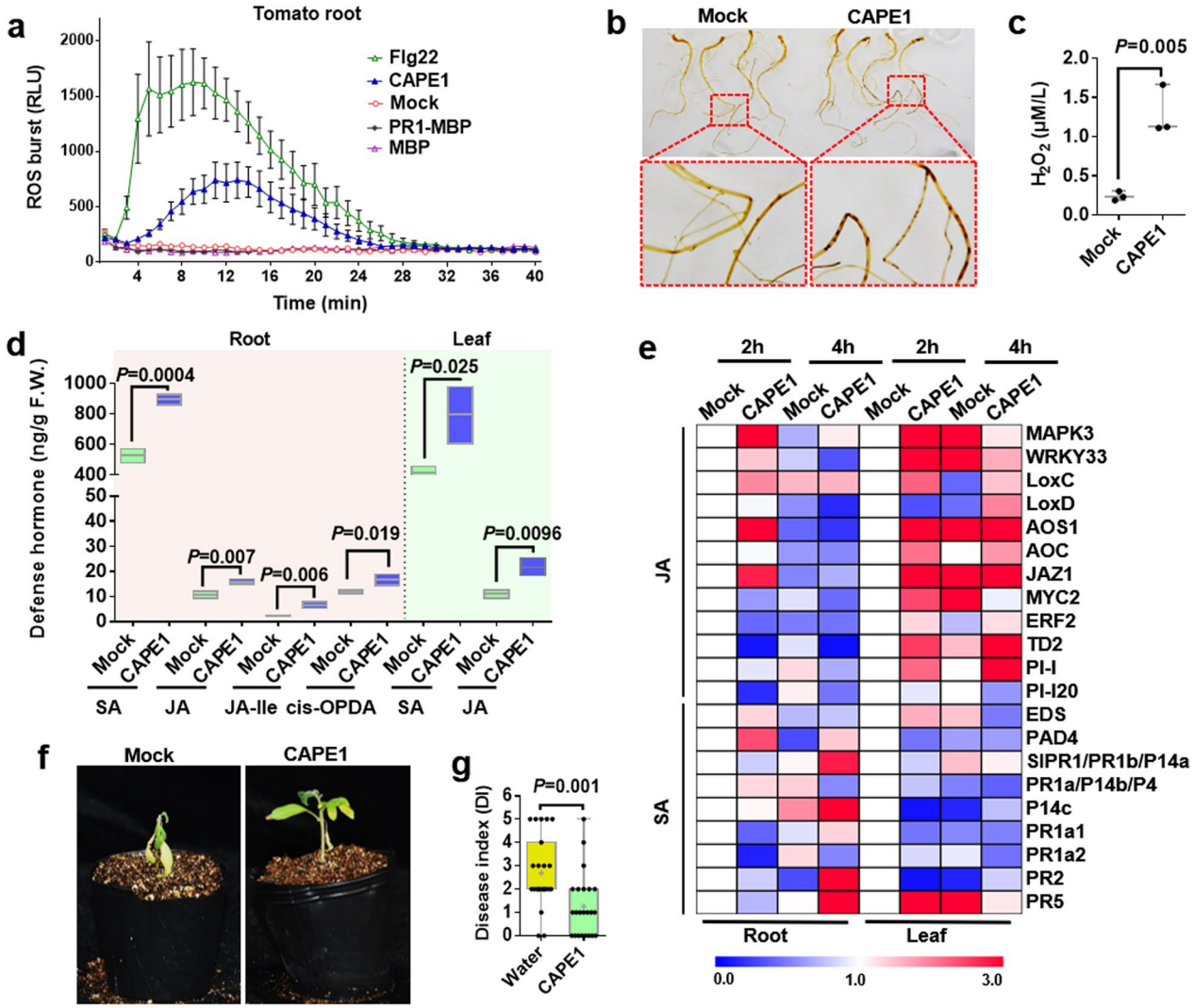

Fig. 5 The CAPE1 peptide of SlPR1 induces root defenses to increase resistance to *Fol* infection. **a** Production of ROS in tomato roots treated with 250 nM CAPE1, SlPR1-MBP, MBP, and 50 nM flg22. The mean values (± SEM) of eight replicates are shown. The experiments were repeated three times, each yielding similar observation. **b** H_2O_2 production in the root tissues was detected after CAPE1 treatment. DAB was used to visualize the H_2O_2 accumulation. The images are representative of the results of three biological repeats. **c** Quantification of H_2O_2 in mock- or CAPE1-treated roots, as in **b**. **d** Production of SA, JA, JA-Ile, and OPDA in the roots after irrigation with or without 250 nM CAPE1. **e** Hierarchical clustering of the abundance of transcripts of SA and JA signaling pathway genes in tomato roots and leaves. At 2 and 4 h after irrigation with a solution of CAPE1, the roots and leaves were collected and ultimately subjected to qRT-PCR. **f** Resistance of tomato seedlings pre-treated with or without CAPE1 prior to *Fol* inoculation. The disease assay was carried out 4 h after application of 250 nM CAPE1 peptide to the tomato roots. **g** Disease index at 14 dpi of 20 plants shown in **f**. For **c**, **d**, and **g**, statistical significance was revealed by Student's *t*-test. The *P* values are shown

SlPR1 is effective against the leaf pathogen *Botrytis cinerea* through CAPE1

To determine whether SlPR1-mediated resistance was conserved in tomato resistance, we measured its expression levels by qRT-PCR in the leaf against necrotrophic pathogen *B. cinerea*. As shown in Additional file 2: Figure S5a and b, the transcripts of *SlPR1* in the leaves were significantly accumulated in response to pathogen inoculation. To determine whether the CAPE1 peptide contributes to tomato resistance to *B. cinerea*, tomato leaves treated with or without synthetic CAPE1 were inoculated with the pathogen. As shown in Additional file 2: Figure S5c, pretreatment with CAPE1 effectively suppressed pathogen invasion, indicating that there is an important role of the CAPE1 peptide in the defense against *B. cinerea*. Furthermore, overexpression of SlPR1 significantly increased the resistance of tomato to *Fol*; however, $^{\Delta CAPE1}$SlPR1 plants displayed disease resistance

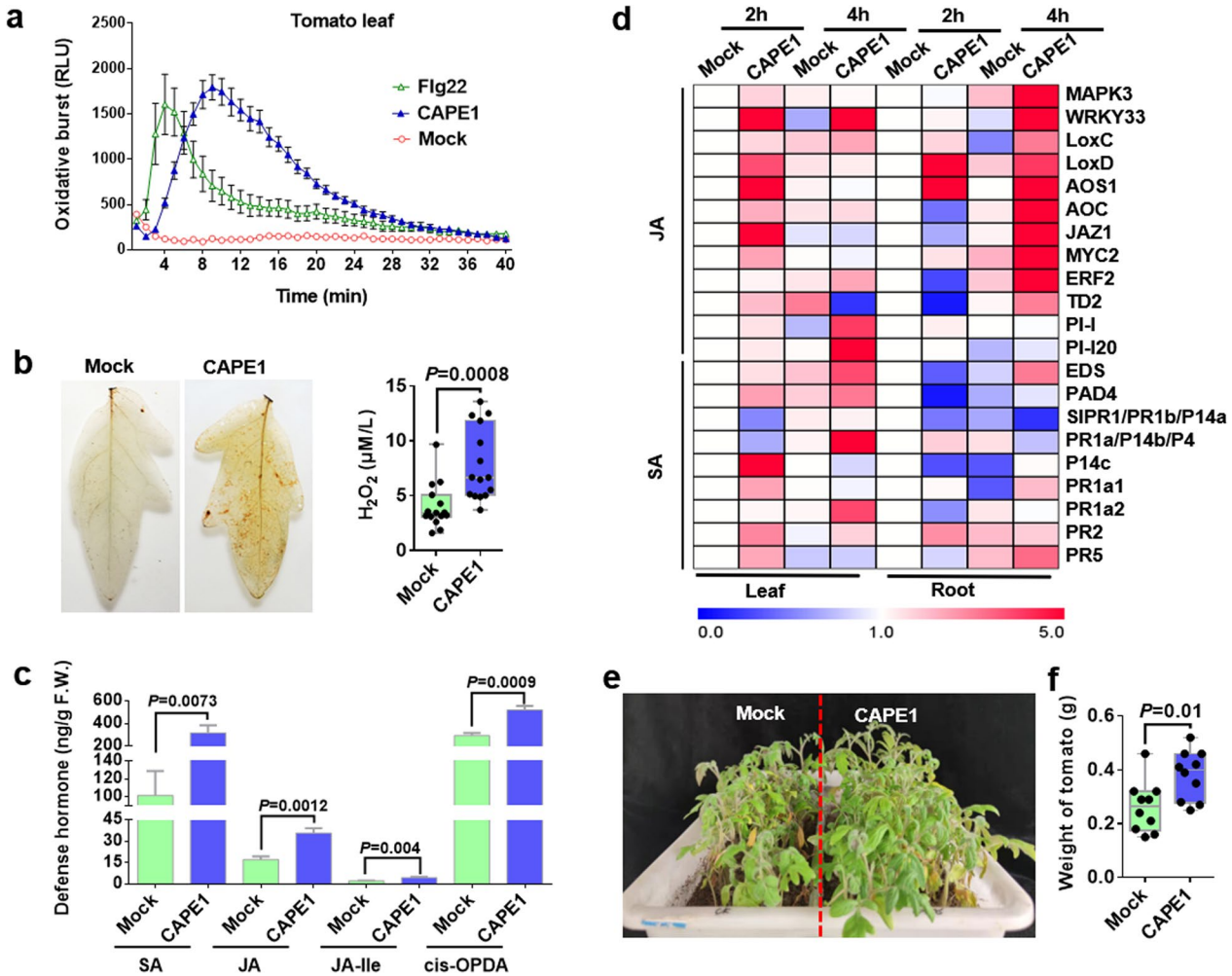

Fig. 6 The CAPE1 peptide actives tomato leaf defense and systemic resistance. **a** Production of ROS in tomato leaves treated with 250 nM CAPE1 or 50 nM flg22. The mean values (±SEM) of eight replicates are shown. The experiments were repeated three times with similar results. **b** CAPE1 induced leaf H_2O_2 production. Detached tomato leaves were inoculated with water (mock) or 250 nM CAPE1 for 4 h. DAB staining was used to visualize H_2O_2 accumulation. The images are representative of the results of three biological repeats (left panel), and the amount of H_2O_2 was also quantified (right panel). **c** The levels of SA and JA in tomato leaves treated with CAPE1. The tomato leaves were sprayed with 250 nM CAPE1 or water (mock), and after 4 h, the content of SA and JA in leaves was quantified. **d** Hierarchical clustering of the abundance of transcripts of SA or JA signaling pathway genes in tomato leaves and roots. After CAPE1 pretreatment for 2 and 4 h, the leaves and roots were collected and subjected to qRT-PCR assays. **e** *Fol* resistance of tomato plants whose leaves were sprayed with a CAPE1 solution. Root inoculation was carried out 4 h after application of 250 nM synthetic CAPE1 or water (mock) to the tomato leaves. The disease symptoms were observed at 10 dpi. **f** The fresh weight of 10 tomato plants shown in **e** was measured at 10 dpi. Statistical significance was determined by Student's *t*-test. The *P* values are shown

similar to that of wild-type plants (Additional file 2: Figure S5d). The microbial growth curve assays showed that MBP-SlPR1 exerted no significant inhibitory activity on *B. cinerea* growth (Additional file 2: Figure S5e). These findings revealed that *SlPR1* also responded to the leaf pathogen *B. cinerea* and contributed to the resistance through CAPE1.

Based on the above data, we proposed a model for how tomato activates early immunity to the pathogen *Fol* (Fig. 7). In response to *Fol* infection, the expression levels of genes involved in multiple defense pathways, mainly the PTI and ETI signaling pathways and the secondary metabolism pathway, are increased. The metabolites galangin and quercetin are effective against *Fol* growth and increase the resistance to *Fol* infection in tomato. In addition, the most significantly upregulated defense-related gene, *SlPR1*, could increase the resistance by activating a series of cellular immune response pathways via the C-terminal CAPE1 peptide of the SlPR1 protein. In particular, CAPE1 could effectively induce SAR to increase host resistance. Overall, these results revealed key defense-related events in tomato plants infected with

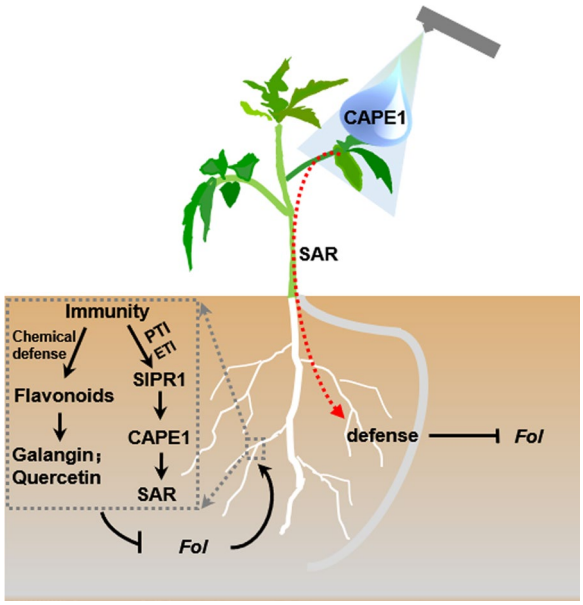

Fig. 7 Model for key immune events occurring in tomato in response to early *Fol* infection and application of CAPE1-mediated systemic resistance for tomato disease control

Fol and provided new insight into exploiting these events to control soil-borne diseases.

Discussion

Plants have evolved a genetically imprinted innate immune that can be activated in preparation for challenge by pathogenic organisms (Zipfel 2008). In our previous studies, we identified 32 candidate effectors that are secreted by *Fol* and provided the clues in the establishment of early *Fol* infection (Li et al. 2020). However, knowledge of the corresponding immune response of tomato against *Fol* during initial infection stages is limited. In this study, the dynamic profiles of the tomato transcriptome during early infection stages were comparatively assayed. Based on the results of a KEGG analysis, seven important pathways were uniquely adapted during the tomato-*Fol* interaction. These pathways were mainly involved in immune signaling and metabolite-dependent chemical defense. Taken together, these findings suggested that early resistance to *Fol* was effectively activated in tomato, which greatly expands our understanding of early immunity in tomato at the transcriptomic level.

Constituting the main chemical defense-related compounds in plants, many phenylpropanoid and flavonoid compounds are essential in the responses to disease resistance (Zaynab et al. 2018; Long et al. 2019; Sharma et al. 2020). For example, plants that accumulate phenylpropanoid coniferin have been shown to display enhanced resistance to the soil-borne vascular pathogen *Verticillium longisporum*; however, coniferin did not seem to affect fungal growth in vitro (König et al. 2014). Similarly, coniferin showed no inhibitory activity on *Fol*. One explanation is that coniferin might increase the contents of other soluble phenylpropanoids to contribute to its perceived role in resistance to pathogen infection (König et al. 2014). Lignin, which is deposited in the secondary cell wall of cells, plays important role in vascular defense to pathogens (Bagniewska-Zadworna et al. 2014; Lin et al. 2022). The upregulation of lignin-related genes in tomato roots indicates that these genes have potential role in early resistance to *Fol*. However, the synthesis of lignin and sodium lignosulfonate showed no direct inhibition on *Fol* growth. Therefore, lignin might function mainly by preventing pathogen from entering physically or increasing root strength to alleviate *Fol* infection (Bagniewska-Zadworna et al. 2014; Lin et al. 2022).

Flavonoids are widely distributed in plants and have a broad range of antimicrobial effects (Morkunas et al. 2005; Echeverría et al. 2017; Ullah et al. 2017; Katsumata et al. 2018; Long et al. 2019). As flavonoid synthesis involves some common enzymes, it is difficult to identify the metabolites that truly accumulated according to our transcriptomic data. Thus, five possible flavonoids were selected to evaluate their antifungal activity. Although no inhibitory activity was observed for pinostrobin, myricetin or homoeriodictyol, we cannot exclude the possibility that these compounds function as precursors for other antifungal flavonoids, which may contribute to the increased resistance to *Fol*. In addition, recent reports have revealed that flavonoids function in early signaling events to chemically recruit specialized associated microbiota as a confrontation strategy to pathogen protection (Berendsen et al. 2012; Wen et al. 2021; Yin et al. 2021). Therefore, flavonoids without antifungal activity might function in recruiting rhizosphere microbes to increase disease resistance. The antibacterial activities of the compounds galangin and quercetin have been reported by the use of different *Staphylococcus aureus* strains (Chung et al. 2011). Here, we report the antifungal activities of galangin and quercetin against *Fol*. In fact, galangin and quercetin were the flavonoids most likely to accumulate in response to *Fol* infection, as more integral genes involved in their synthesis pathways were upregulated. These findings suggest that flavonoids function in early immunity against *Fol* invasion in tomato and that galangin and quercetin might be the important members of the main chemical defense metabolites such as phytoalexins in tomato (Ahuja et al. 2012).

Recent studies show that PRR- and NLR-mediated immunity can enhance each other and are codependent, and mutually potentiated PRRs and NLRs lead to increased calcium influx, ROS production, and SA

accumulation (Ngou et al. 2021, 2022; Pruitt et al. 2021; Tian et al. 2021; Yuan et al. 2021). In response to *Fol*, the increased transcripts of 12 PRRs and 3 NLRs implicated their potency for enhancing pathogen recognition and induction of downstream defenses. Moreover, more than 30% of the genes in the PTI and ETI pathways were found to induce fourfold in response to *Fol* infection, implying that there is an activation of the two-tier innate immune system. These findings greatly expand our understanding of early immunity in tomato and provide valuable resources for genetic improvement against tomato disease, such as the most prominent resistance protein, SlPR1. Although the function of PR1 in the development and stress response is largely unknown, the importance of PR1 is underscored by the fact that no *PR1* knockout mutants is reported in tomato databases (Li et al. 2022) or any other plant databases (Lincoln et al. 2018).

PR1s is typically considered to be related to defense against biotrophs or hemi-biotrophs (Glazebrook 2005); however, only a few reports have addressed the role of these proteins during biotic interactions (Sung et al. 2021). Although the PR1 homolog P14c effectively inhibits *Phytophthora* species, the growth of the pathogenic fungi *Aspergillus niger* or *B. cinerea* was impervious to P14c (Gamir et al. 2016; Breen et al. 2017). SlPR1 has conserved motifs involved in the inhibitory activity of P14c and PR1a (Breen et al. 2017); however, no antimicrobial activity for SlPR1 was detected against *Fol* or *B. cinerea*. We also failed to observe any disease resistance when CAPE truncated SlPR1 was overexpressed in tomato (Li et al. 2022). Collectively, these data suggests that the SlPR1-dependent repression effects on *Fol* growth in planta might be not a result of antifungal activity. Similarly, the SlPR1 ortholog TaPR1 from wheat exerted neither antimicrobial nor sterol-binding activity (Sung et al. 2021). Instead, an SlPR1-overexpressing line exhibited a putative C-terminal CAPE1-GFP fusion protein, indicating that CAPE1 was released in tomato in response to *Fol* infection (Li et al. 2022). Therefore, we focused on the clarification of the PR1 C-terminal peptide as an inducer of defense responses.

Functionally, CAPE1 functions as a signaling molecule to activate root or leaf cellular responses and repress the infection of *Fol* and *B. cinerea*, respectively. Similarly, CAPE1 was previously reported to increase the resistance to the pathogenic bacteria *Pseudomonas syringae* pv. tomato Pst DC3000, and its homologous peptides from AtPR1 in *Arabidopsis thaliana* or TaPR-1 in wheat were found to be bioactive (Chen et al. 2014; Sung et al. 2021). These findings indicated that SlPR1 might function importantly in plant defense, which is mainly dependent on its C-terminal peptide CAPE1. To further support it, the putative caspase (a type of cysteine protease that cleaves lysine/arginine) was reported to proteolyze the salicylic acid signaling marker PR1 to produce the cytokine CAPE9 for systemic immunity in Arabidopsis (Chen et al. 2021). In plant, the functional analogs of caspases are annotated as metacaspases. From this transcriptome data, 3/8 metacaspases were significantly upregulated at 2 dpi and 3 dpi (Additional file 1: Tables S8, S9), which might be responsible for the cleavage of CAPE1 peptide from SlPR1. Unsurprisingly, peptide release from precursor proteins can induce host defense signaling. For example, the 23-amino acid peptide AtPep1 released from its precursor protein PROPEP1 result in inducting defense-related genes PDF1.2 and PR1 (Huffaker et al. 2006; Hander et al. 2019). Similarly, the Zip1 peptide released from the PROZIP1 protein can trigger SA-mediated defense in *Zea mays* (Ziemann et al. 2018). Notably, our results showed that the CAPE1 peptide could induce SAR through substantial increases in JA levels and induction of defense signaling-related genes, which might be involved in root growth, defense activation, and biosynthesis of diverse metabolites (e.g., terpenoids and phytoalexins) (Ghorbel et al. 2021). On the one hand, these findings suggested that CAPE1 released from the SlPR1 could be a key inducer to activate JA-mediated systemic disease resistance, which also provided clues about the crosstalk between SA and JA, with focusing on the biological importance of these interactions during host defense.

Conclusions

In this study, tomato employs several sophisticated molecular mechanisms to activate its immune responses against *Fol* infection. These mechanisms mainly include flavonoid-mediated chemical defense induction and 'PTI + ETI'-mediated basal defense induction. In particular, the research described here provides new evidence that the defense signaling peptide CAPE1 from SlPR1 is indeed able to trigger immune responses and systemic resistance. Therefore, exogenous applications of CAPE1 or defense-related metabolites could be used to promote the disease resistance in tomato as part of a pest management strategy. However, unlike the adaptation cost of the constitutive resistance related to inducible resistance, the fitness cost of CAPE1 usually seems to overbalance the cost of pathogen infection. Therefore, the immune signaling molecule CAPE1 applied to increase plant defenses while maintain optimal yield is still under investigation, especially the underlying signal recognition mechanism.

Methods

Plants, fungal strains, and cultural conditions

Wild type tomato (*S. lycopersicum* cv. Alisa Craig [AC]) plants were sown in a soil mixture

(vermiculite:humus = 1:2) and grown in a growth chamber at 28°C with relative humidity of 65% and a 16-h light/8-h dark cycle (Cao et al. 2018). The *SlPR1* transgenic tomato used in this study was the same as those used in our previous study (Li et al. 2022). The standard reference strain Fol4287 of *Fol* (Li et al. 2020) and B05.10 of *B. cinerea* (Yang et al. 2022) were used and cultured on plates of potato dextrose agar (PDA) in an incubator at 25°C. To collect the conidia of *Fol*, 8–10 mycelial colonized agar plugs were cultured in 150 mL of potato dextrose broth (PDB) liquid media with shaking at 200 rpm at 25°C for 14 h. For B05.10, the conidia were collected from 10 days old PDA cultures (Yang et al. 2022). The conidia harvested at the concentration of 5×10^6 spores/mL (Vitale et al. 2019) were used for infection and antifungal assays.

Early infection of *Fol* in tomato roots

To identify the early infection and colonization of *Fol* in tomato roots, we detected *Fol* biomass by PCR. In brief, the collected conidia were resuspended in 300 ml of water at a concentration of 5×10^6 conidia/mL. Three-week-old tomato (20–25 seedlings per point) were inoculated with *Fol* conidia and then kept at 25°C. The plants were harvested at 0, 1, 2, and 3 dpi. All the specimens were washed five times, and the samples were immediately immersed in liquid nitrogen and preserved in the freezer at −80°C for DNA extraction. Then, the *Fol* histone H4-specific gene *FolH4* was used to detect *Fol* invasive colonization by PCR amplification with the primer pairs FolH4-F and FolH4-R (Additional file 1: Table S6). The tomato *SlActin* was used as a reference gene for normalizing the root sample genes.

Transcriptomic analysis

To form RNA-seq data from *Fol*-infected roots, an infection assay was performed as described above. Then, tomato roots were immediately collected after inoculation (0 dpi) and at 1, 2, and 3 dpi with *Fol* conidia. RNA samples were extracted from three biological repeats of each treatment and then used to construct the cDNA library. These constructed libraries were subsequently sequenced using an Illumina NovaSeq platform (Illumina, San Diego, CA, USA) at Personalbio Technology Co., Ltd. (Shanghai, China). Approximately 6 Gb of reads for each sample were obtained. After filtering and removing the low-quality reads by Cutadapt (https://github.com/marcelm/cutadapt/), we mapped the processed reads to the tomato genome GCF_000188115.4_SL3.0 (https://www.ncbi.nlm.nih.gov/genome/?term=Solanum+lycopersicum) via the HISAT2 program (https://github.com/DaehwanKimLab/hisat2). After the alignment with each gene model, we calculated the normalized expression data of each gene using FRPKM values. The differentially expressed genes were selected by DESeq2 in accordance with the criteria of an absolute $\log_2(FC) \geq 1$ and an FDR ≤ 0.05 between any two samples. The Z scores of the subsequent RNA-seq dataset was used to analyze gene expression changes using the ggplot2 package (https://cran.rproject.org/web/packages/ggplot2/), and heatmap is built using the heatmap package (https://cran.rproject.org/web/packages/pheatmap/). For pathway mapping, the KEGG Orthology database was used (http://www.genome.jp/kegg/). Enrichment pathway was analyzed by the clusterProfiler package to test the statistical enrichment of DEGs in the KEGG pathways. To annotate the tomato unique genes, BLASTx algorithm was used to compare the sequence in NCBI nonredundant (Nr) protein database, and the e-value threshold was 10^{-5}.

The PCA results are shown in Additional file 1: Table S7. The FPKM values corresponding to the roots of the *Fol*-inoculated plants and control plants are shown in Additional file 1: Table S8, and the $\log_2(FC)$ values of read counts corresponding to the roots of the *Fol*-inoculated plants and control plants are shown in Additional file 1: Table S9. The Z scores values of RNA-seq data for heatmap are shown in Additional file 1: Table S10, and the results of KEGG pathway analysis are in Additional file 1: Table S2.

RNA extraction and qRT-PCR assays

The qRT-PCR experiments were used to verify the RNA-seq results with independent root samples of *Fol*-inoculated (1, 2, 3, 4 dpi) tomato plants and control roots (0 dpi) under the conditions as same as those used for RNA-seq. The total RNA was isolated from tissue by using TRIzol extraction (Invitrogen) according to the manufacturer's manual. The RNA (2 μg) was reverse transcribed into cDNA using the PrimeScript RT Reagent Kit (TaKaRa). Transcription profiling was performed using a 2 × M5 HiPer SYBR Premix ExTaq Kit (Mei5bio) and a LightCycler® 96 (Roche) real-time PCR detection system. Relative expression level of the genes was determined using the $2^{-\Delta\Delta ct}$ method (Li et al. 2018).

For qRT-PCR of *SlPR1* in response to *B. cinerea* infection, tomato leaves were fully covered with 5×10^6 spores/mL by spraying. Then, the leaves were harvested at 0, 4, 8, 12, 24, and 48 hpi for RNA isolation and qRT-PCR as described above. The semi-qRT-PCR technique used was the same as that described previously (Li et al. 2016).

For qRT-PCR detection of the SA- and JA-related genes in response to the CAPE1 peptide, the tomato leaves were fully covered with 250 nM CAPE1 by spraying. Then, the leaves and roots were collected at 2 and 4 h after CAPE1 treatment, respectively. The tomato roots were irrigated with 200 mL of 250 nM CAPE1. Then, the

leaves and roots were collected at 2 and 4 h after CAPE1 treatment for qRT-PCR detection. RNA extraction and cDNA synthesis were carried out as above. A total of 21 SA- and JA signaling pathway genes were selected, and their expression profiles were verified by qRT-PCR as above. The genes were normalized to the *SlActin* gene, and the primers used for qRT-PCR are shown in Additional file 1: Table S6.

Antimicrobial activity of phenylpropanoid and flavonoid metabolites

The synthetic drug sodium lignosulfonate (CAS 8061-51-6, Macklin, Shanghai, China) was dissolved in ddH_2O to a concentration of 125 μg/L. Coniferin (CAS 531-29-3, Chengdu Biopurify Phytochemicals, Ltd., Chengdu, China), homoeriodictyol (CAS 446-71-9, Macklin, Shanghai, China), and quercetin (CAS 117-39-5, Macklin, Shanghai, China) were dissolved in ethanol to a concentration of 125 μg/L. Lignin (CAS 9005-53-2, Macklin, Shanghai, China), pinostrobin (CAS 480-37-5, Chengdu Biopurify Phytochemicals, Ltd., Chengdu, China), galangin (CAS 548-83-4, Macklin, Shanghai, China), and myricetin (CAS 529-44-2, Macklin, Shanghai, China) were dissolved in dimethyl sulfoxide (DMSO) to the concentration of 125 μg/L. These selected drugs mimic metabolism and were used to evaluate antimicrobial activity. In brief, a 1×10^5 spores/mL in a total volume of 100 μL that consists of 5% liquid YEPD medium and 125 μg/mL or 62.5 μg/mL of the indicated drugs were cultured in a 96-well microtiter plate at 25°C with shaking at 100 rpm. The quantification curve of mycelia growth was generated by measuring the absorbance at 600 nm using a SPECTROstar Omega plate reader (BMG LABTECH). ddH_2O, ethanol, or DMSO were used as solvent controls based on the dissolution properties of the drugs.

For inhibition assays of the plates, agar plugs with fresh *Fol* strains were inoculated onto plates of PDA that included 62.5 μg/mL galangin or quercetin. PDA media supplemented with the solvent DMSO or ethanol was used as controls. Then the diameters of mycelium colony were determined at 3 dpi.

Disease assays

Pathogenicity assays of *Fol* were carried out using the root-dip method with moderate modification (Di et al. 2016; Zhang et al. 2021). Briefly, 14-day-old tomato plants were uprooted from the soil and then inoculated with a conidia suspension (5×10^6 spores/mL) or were mock treated (no spores) for 10 min, then the tomato seedlings were repotted and maintained at 28°C. Two weeks later, the disease symptoms of treated tomato were evaluated with a disease index ranging from 0–5 as described previously (Li et al. 2022).

The synthetic CAPE1 peptide (PVGNWIGQRPY; 98.48% pure) was purchased from GL Biochem. For the *Fusarium* wilt disease resistance test of CAPE1 in the roots, the tomato seedlings were incubated with 250 nM synthetic CAPE1 for 20 min followed by pathogen inoculation. To induce systemic resistance to *Fol*, two groups of tomato leaves were sprayed with either water or 250 nM CAPE1. Four hours later, the *Fol* conidia were then used for inoculation assays on the treated tomato seedlings.

For the *Fusarium* wilt disease resistance test of the flavonoid drugs, the tomato seedlings were treated with 62.5 μg/mL galangin or quercetin for 20 min followed by pathogen inoculation as described above.

For the *B. cinerea* disease resistance test of CAPE1, tomato leaves were sprayed with 250 nM CAPE1 peptide 4 h prior to pathogen inoculation as reported previously (Yang et al. 2022). The pathogenicity test of *SlPR1* transgenic tomato was performed in the same manner as described above. The lesion areas were measured at 36 hpi.

SlPR1 purification and antifungal assays

SlPR1 gene sequences lacking its N-terminal 19-amino acids were constructed into a pExp-his-xMBP-TEV vector via the homologous cloning experiment with the primers listed in Additional file 1: Table S6. The fused His-MBP-SlPR1 proteins were expressed in *E. coli* BL21 strain and purified by the method described previously (Li et al. 2022). Briefly, the cells were lysed with the buffer containing 500 mM NaCl, 20 mM Tris–HCl, 20 mM imidazole and 1 mM phenylmethylsulfonyl fluoride (PMSF) in a microfluidizer. The His-tagged SlPR1 at its N-terminus were then purified using Ni-nitrilotriacetic acid (Ni–NTA) resin (Qiagen) according to the manufacturer's manual. Then proteins were eluted with elution buffer (500 mM NaCl, 300 mM imidazole, and 20 mM Tris–HCl (pH 8.0)), and the protein fraction was desalted on a Sephadex G-25 desalting column PD-10, GE Healthcare) flow-through with 50 mM Tris–HCl (pH 8). The purified protein was concentrated with a 10 kDa MWCO Amicon Ultra Centrifugal Filter (Merck Millipore) and quantified with the Omni-Easy™ Instant BCA Protein Assay Kit (Epizyme). Subsequently, the protein was verified by Coomassie-stained SDS-PAGE and then for antimicrobial analysis.

To determine the antimicrobial activity of recombinant MBP-SlPR1 protein, 1×10^5 spores/mL of *Fol* or *B. cinerea* in a total volume of 100 μL consisting of 5% liquid YEPD media and 200 μg/mL purified SlPR1 fusion protein were incubated in a 96-well plate. A hyphal growth quantification curve was generated according to the

inhibition assays of the abovementioned drugs. Purified MBP protein was employed as a control. For the inhibition assays on plates, agar plugs with fresh *Fol* strains were inoculated onto plates of PDA that included 200 μg/mL MBP-SlPR1 or MBP. The diameters of mycelial colony were measured at 3 dpi.

Measurement of ROS

ROS burst was monitored with a luminol/peroxidase-based assay as described previously (Sang and Macho 2017). In brief, sterile H_2O-balanced tomato leaf discs or two-week-old tomato roots in a 96-well white plate were replaced with a luminol (100 μM/L)/peroxidase (20 μg/mL) reaction buffer that included sterilized water, 50 nM flg22 (Genscript Biotech, China), or 250 nM synthesized CAPE1 protein. The luminescence was subsequently monitored using a Varioskan LUX reader (Thermo Scientific, USA).

3′-Diaminobenzidine (DAB) staining and H_2O_2 quantification

The detection of H_2O_2 was conducted using DAB, which was obtained from Sigma–Aldrich. Briefly, detached tomato roots or leaves were incubated with sterilized water or 250 nM synthetic CAPE1 for 4 h, after which the tomato tissues were resuspended in solution buffer (pH = 3.8) containing 1 mg/mL DAB and incubated in the dark for 8 h at room temperature. Subsequently, the tomato samples were bleached with 95% ethanol until the roots or leaves became colorless (Yang et al. 2022).

The H_2O_2 content was monitored with a H_2O_2 detection kit (Beyotime, S0038) based on the manufacturer's protocol. Briefly, 10 mg of tomato tissue was homogenized together with 200 μL of lysate and centrifuged at 4°C for obtaining the supernatant component. The reaction buffer included 50 μL of supernatant and 100 μL of H_2O_2 detection reagent and was incubated at 24°C for 0.5 h. Then, the absorbance of the mixture was immediately monitored using a spectrometer at 560 nm. Absorbance values were calibrated to a standard curve generated with known concentrations of H_2O_2.

Determination of endogenous hormone contents

To quantify the contents of SA and JA that accumulated in response to the CAPE1 peptide, tomato leaves were collected 4 h after they were sprayed with 250 nM CAPE1 or mocked control (sterilized water). Similarly, the tomato roots were collected 4 h after the plants were irrigated with 250 nM CAPE1 or sterilized water. Approximately 0.1 g of fresh tissue samples were prepared for hormone extractions and quantification as described previously (Hackenberg and Pandey 2014). The contents of SA, JA, the jasmonoyl-isoleucine (JA-Ile) conjugate, and the JA precursor cis-(+)-12-oxo-phytodienoic acid (OPDA) were assayed via liquid chromatography-selected reaction monitoring–mass spectrometry (LC-SRM-MS) at APT (Shanghai, China). The content of the hormones were measured in three technical replicates via multiple reaction monitoring transitions and quantified with standard samples. Each sample was measured with three biological replicates.

Bioinformatic analyses

Multiple amino acids sequences alignments were carried out using DNAMAN 6 software (Li et al. 2022). 3D structural models of the SlPR1 proteins were constructed using the online server Iterative Threading ASSEmbly Refinement (I-TASSER) (Yang and Zhang 2015). BLAST-based KEGG Orthology annotations and KEGG mapping were performed to analyze the phenylpropanoid and flavonoid biosynthesis pathways through the online server (https://www.kegg.jp/kegg/kegg1a.html). Original Sanger sequencing traces were opened with SnapGene software.

Statistical analysis

Data were imported to the software GraphPad Prism version 6 (La Jolla, CA, USA) to create all graphs. Statistical analyses were performed by one-way analysis of variance (ANOVA) or the unpaired Student's *t*-test.

Abbreviations

ABA	Abscisic acid
ANOVA	One-way analysis of variance
ATP	Adenosine triphosphate
BR	Brassinosteroids
CaM	Calmodulin
CAPE1	CAP-derived peptide 1
CAS	Chemical abstracts service
CBB	Coomassie brilliant blue
CHI	Chalcone isomerase
CHS	Chalcone synthase
Cis-OPDA	Cis-(+)-12-oxo-phytodienoic acid
CNG	Cyclic nucleotide-gated
CPKs	Calcium-dependent protein kinases
DAMPs	Damage-associated molecular patterns
DEGs	Differentially expressed genes
DMSO	Dimethyl sulfoxide
ERB	Ethylene responsive element binding protein
ERF	Ethylene-responsive factor
ET	Ethylene
ETI	Effector-triggered immunity
F3H	Flavonoid-3-hydroxylase
FC	Fold-change
FDR	False discovery rate
FLS	Flavonol synthase
Fol	*Fusarium oxysporum* F. sp. *lycopersici*
FRPKM	Fragments per kilobase of transcript per million mapped reads
GA	Gibberellic acid
IAA	Indoleacetic acid
JA	Jasmonic acid
JA-Ile	JA-isoleucine
KEGG	Kyoto encyclopedia of genes and genomes
LC-SRM-MS	Liquid chromatography-selected reaction monitoring-mass spectrometry

LRR	Leucine rich repeat
MAMPs	Microbe-associated molecular patterns
MAPK	Mitogen-activated protein kinase
MBP	Maltose binding protein
NADPH	Nicotinamide adenine dinucleotide phosphate
NLRs	Nucleotide-binding leucine-rich repeat receptors
PAMPs	Pathogen-associated molecular patterns
PCA	Principal component analysis
PDA	Potato dextrose agar
PDB	Potato dextrose broth
PRRs	Pattern recognition receptors
PRs	Pathogenesis-related proteins
Pst	*Pseudomonas syringae* Pv. tomato
PTI	Pattern-triggered immunity
RBOH	Respiratory burst oxidase homolog
RLCK	Receptor-like cytoplasmic kinase
RLK	Receptor-like kinases
RLP	Receptor-like proteins
RNA-seq	RNA sequencing
ROS	Reactive oxygen species
R proteins	Resistance proteins
SA	Salicylic acid
SAR	Systemic acquired resistance
SDS-PAGE	Sodium dodecyl sulphate–polyacrylamide gel electrophoresis
TFs	Transcription factors

Supplementary Information

The online version contains supplementary material available at https://doi.org/10.1186/s42483-023-00176-y.

Additional file 1: Table S1. Mapping information of transcript reads. **Table S2.** KEGG analysis of different expressed genes. **Table S3.** Summary of PTI and ETI related DEGs. **Table S4.** PTI and ETI related DEGs with a $\log_2$greater than 2. **Table S5.** Transcriptomic data of the genes encoding the enzymes involved in the biosynthesis of flavonoids from phenylalanine. **Table S6.** Primers used in this study. **Table S7.** Principal Component Analysisdata of the RNA-seq data sets. **Table S8.** Expression data of the RNA-seq data sets. **Table S9.** The $\log_2$values of the RNA-seq data sets. **Table S10.** Z scores of RNA-seq data sets for heatmap.

Additional file 2: Figure S1. Analysis of significant DEGs. **Figure S2.** Venn diagram and gene expression patterns of DEGs. **Figure S3.** Schematic representation of DEGs involved in plant immunity. **Figure S4.** Sequence alignment of SlPR1, tobacco PR1a and tomato P14c according to DNAMAN 6.0. **Figure S5.** The CAPE1 peptide of SlPR1 contributes to tomato resistance to *B. cinerea* B05.10.

Acknowledgements
Not applicable.

Authors' contributions
JL and CW carried out the experiments. LY, FQ, YL, YZ, and SL performed technical supports and statistical analysis. WL, LS, and JL initiated the project, designed the experiments, analyzed the data, and provided funding. JL, LS, and WL wrote the manuscript with inputs from all the authors. All authors read and approved the final manuscript.

Funding
This study was financially supported by the National Natural Science Foundation of China (32272489, 31972213), the Shandong Province 'Double-Hundred Talent Plan' (WST2018008), and the Taishan Scholar Construction Foundation of Shandong Province (tshw20130963).

Availability of data and materials
The datasets used and/or analyzed during the current study are available from the corresponding author on reasonable request. The datasets generated and/or analyzed during the current study are available in the NCBI repository, https://www.ncbi.nlm.nih.gov/sra/PRJNA909936.

Declarations

Ethics approval and consent to participate
Not applicable.

Consent for publication
Not applicable.

Competing interests
The authors declare that they have no competing interests.

Received: 28 December 2022 Accepted: 11 April 2023
Published online: 26 May 2023

References

Ahuja I, Kissen R, Bones AM. Phytoalexins in defense against pathogens. Trends Plant Sci. 2012;17(2):73–90. https://doi.org/10.1016/j.tplants.2011.11.002.

Bagniewska-Zadworna A, Barakat A, Łakomy P, Smoliński DJ, Zadworny M. Lignin and lignans in plant defence: Insight from expression profiling of cinnamyl alcohol dehydrogenase genes during development and following fungal infection in *Populus*. Plant Sci. 2014;229:111–21. https://doi.org/10.1016/j.plantsci.2014.08.015.

Berendsen RL, Pieterse CMJ, Bakker PAHM. The rhizosphere microbiome and plant health. Trends Plant Sci. 2012;17(8):478–86. https://doi.org/10.1016/j.tplants.2012.04.001.

Breen S, Williams SJ, Outram M, Kobe B, Solomon PS. Emerging insights into the functions of pathogenesis-related protein 1. Trends Plant Sci. 2017;22(10):871–9. https://doi.org/10.1016/j.tplants.2017.06.013.

Cao L, Blekemolen MC, Tintor N, Cornelissen BJC, Takken FLW. The *Fusarium oxysporum* Avr2-Six5 effector pair alters plasmodesmatal exclusion selectivity to facilitate cell-to-cell movement of Avr2. Mol Plant. 2018;11(5):691–705. https://doi.org/10.1016/j.molp.2018.02.011.

Chen Y-L, Lee C-Y, Cheng K-T, Chang W-H, Huang R-N, Nam HG, et al. Quantitative peptidomics study reveals that a wound-induced peptide from PR-1 regulates immune signaling in tomato. Plant Cell. 2014;26(10):4135–48. https://doi.org/10.1105/tpc.114.131185.

Chen YL, Lin FW, Cheng KT, Wang HY, Chen YR. XCP1 is a caspase that proteolyzes pathogenesis-related protein 1 to produce the cytokine CAPE9 for systemic immunity in Arabidopsis. Res Square. 2021. https://doi.org/10.21203/rs.3.rs-155784/v1.

Choudhary V, Schneiter R. Pathogen-Related Yeast (PRY) proteins and members of the CAP superfamily are secreted sterol-binding proteins. Proc Natl Acad Sci U S A. 2012;109(42):16882–7. https://doi.org/10.1073/pnas.1209086109.

Chung PY, Navaratnam P, Chung LY. Synergistic antimicrobial activity between pentacyclic triterpenoids and antibiotics against *Staphylococcus aureus* strains. Ann Clin Microbiol Antimicrob. 2011;10(1):25. https://doi.org/10.1186/1476-0711-10-25.

Dangl JL, Horvath DM, Staskawicz BJ. Pivoting the plant immune system from dissection to deployment. Science. 2013;341(6147):746–51. https://doi.org/10.1126/science.1236011.

Di X, Gomila J, Ma L, van den Burg HA, Takken FLW. Uptake of the *Fusarium* effector Avr2 by tomato is not a cell autonomous event. Front Plant Sci. 2016;7:1915. https://doi.org/10.3389/fpls.2016.01915.

Dixon RA. Natural products and plant disease resistance. Nature. 2001;411(6839):843–7. https://doi.org/10.1038/35081178.

Echeverría J, Opazo J, Mendoza L, Urzúa A, Wilkens M. Structure-activity and lipophilicity relationships of selected antibacterial natural flavones and flavanones of Chilean flora. Molecules. 2017;22(4):E608. https://doi.org/10.3390/molecules22040608.

Fu ZQ, Dong X. Systemic acquired resistance: turning local infection into global defense. Annu Rev Plant Biol. 2013;64(1):839–63. https://doi.org/10.1146/annurev-arplant-042811-105606.

Gamir J, Darwiche R, van't Hof P, Choudhary V, Stumpe M, Schneiter R, et al. The sterol-binding activity of pathogenesis-related protein 1 reveals the mode of action of an antimicrobial protein. Plant J. 2016;89(3):502–9. https://doi.org/10.1111/tpj.13398.

Geng D, Shen X, Xie Y, Yang Y, Bian R, Gao Y, et al. Regulation of phenylpropanoid biosynthesis by MdMYB88 and MdMYB124 contributes to pathogen and drought resistance in apple. Hortic Res. 2020. https://doi.org/10.1038/s41438-020-0324-2.

Ghorbel M, Brini F, Sharma A, Landi M. Role of jasmonic acid in plants: the molecular point of view. Plant Cell Rep. 2021;40(8):1471–94. https://doi.org/10.1007/s00299-021-02687-4.

Glazebrook J. Contrasting mechanisms of defense against biotrophic and necrotrophic pathogens. Annu Rev Phytopathol. 2005;43:205–27. https://doi.org/10.1146/annurev.phyto.43.040204.135923.

Hackenberg D, Pandey S. Heterotrimeric G-proteins in green algae. Plant Signal Behav. 2014;9(4):e28457. https://doi.org/10.4161/psb.28457.

Hander T, Fernández-Fernández ÁD, Kumpf RP, Willems P, Schatowitz H, Rombaut D, et al. Damage on plants activates Ca^{2+}-dependent metacaspases for release of immunomodulatory peptides. Science. 2019;363(6433):eaar7486. https://doi.org/10.1126/science.aar7486.

Huffaker A, Pearce G, Ryan CA. An endogenous peptide signal in *Arabidopsis* activates components of the innate immune response. Proc Natl Acad Sci. 2006;103(26):10098–103. https://doi.org/10.1073/pnas.0603727103.

Kamle M, Borah R, Bora H, Jaiswal AK, Singh RK, Kumar P. Systemic acquired resistance (SAR) and induced systemic resistance (ISR): role and mechanism of action against phytopathogens. In: Upadhyay RS, Sharma GD, Manoharachary C, Gupta VK, Hesham AE-L, editors. Fungal biotechnology and bioengineering. Cham: Springer; 2020. p. 457–70. https://doi.org/10.1007/978-3-030-41870-0_20.

Katsumata S, Toshima H, Hasegawa M. Xylosylated detoxification of the rice flavonoid phytoalexin sakuranetin by the rice sheath blight fungus *Rhizoctonia solani*. Molecules. 2018;23(2):276. https://doi.org/10.3390/molecules23020276.

Kong X, Zhang C, Zheng H, Sun M, Zhang F, Zhang M, et al. Antagonistic interaction between auxin and SA signaling pathways regulates bacterial infection through lateral root in *Arabidopsis*. Cell Rep. 2020;32(8):108060. https://doi.org/10.1016/j.celrep.2020.108060.

König S, Feussner K, Kaever A, Landesfeind M, Thurow C, Karlovsky P, et al. Soluble phenylpropanoids are involved in the defense response of Arabidopsis against *Verticillium longisporum*. New Phytol. 2014;202(3):823–37. https://doi.org/10.1111/nph.12709.

Li J, Yu G, Sun X, Zhang X, Liu J, Pan H. AcEBP1, an ErbB3-Binding Protein (EBP1) from halophyte *Atriplex canescens*, negatively regulates cell growth and stress responses in *Arabidopsis*. Plant Sci. 2016;248:64–74. https://doi.org/10.1016/j.plantsci.2016.04.011.

Li J, Mu W, Veluchamy S, Liu Y, Zhang Y, Pan H, et al. The GATA-type IVb zinc-finger transcription factor SsNsd1 regulates asexual–sexual development and appressoria formation in *Sclerotinia sclerotiorum*. Mol Plant Pathol. 2018;19(7):1679–89. https://doi.org/10.1111/mpp.12651.

Li J, Gao M, Gabriel DW, Liang W, Song L. Secretome-wide analysis of lysine acetylation in *Fusarium oxysporum* f. sp. *lycopersici* provides novel insights into infection-related proteins. Front Microbiol. 2020;11:559440. https://doi.org/10.3389/fmicb.2020.559440.

Li J, Wang C, Liang W, Liu S. Rhizosphere microbiome: the emerging barrier in plant-pathogen interactions. Front Microbiol. 2021;12(3381):772420. https://doi.org/10.3389/fmicb.2021.772420.

Li J, Ma X, Wang C, Liu S, Yu G, Gao M, et al. Acetylation of a fungal effector that translocates host PR1 facilitates virulence. Elife. 2022;11:e82628. https://doi.org/10.7554/eLife.82628.

Lin H, Wang M, Chen Y, Nomura K, Hui S, Gui J, et al. An MKP-MAPK protein phosphorylation cascade controls vascular immunity in plants. Sci Adv. 2022;8(10):eabg8723. https://doi.org/10.1126/sciadv.abg8723.

Lincoln JE, Sanchez JP, Zumstein K, Gilchrist DG. Plant and animal PR1 family members inhibit programmed cell death and suppress bacterial pathogens in plant tissues. Mol Plant Pathol. 2018;19(9):2111–23. https://doi.org/10.1111/mpp.12685.

Liu X, Zhang P, Zhao Q, Huang AC. Making small molecules in plants: a chassis for synthetic biology-based production of plant natural products. J Integr Plant Biol. 2023;65(2):417–43. https://doi.org/10.1111/jipb.13330.

Long L, Liu J, Gao Y, Xu F-C, Zhao J-R, Li B, et al. Flavonoid accumulation in spontaneous cotton mutant results in red coloration and enhanced disease resistance. Plant Physiol Biochem. 2019;143:40–9. https://doi.org/10.1016/j.plaphy.2019.08.021.

Michielse CB, Rep M. Pathogen profile update: *Fusarium oxysporum*. Mol Plant Pathol. 2009;10(3):311–24. https://doi.org/10.1111/j.1364-3703.2009.00538.x.

Morkunas I, Marczak Ł, Stachowiak J, Stobiecki M. Sucrose-induced lupine defense against *Fusarium oxysporum*: Sucrose-stimulated accumulation of isoflavonoids as a defense response of lupine to *Fusarium oxysporum*. Plant Physiol Biochem. 2005;43(4):363–73. https://doi.org/10.1016/j.plaphy.2005.02.011.

Ngou BPM, Ahn H-K, Ding P, Jones JDG. Mutual potentiation of plant immunity by cell-surface and intracellular receptors. Nature. 2021. https://doi.org/10.1038/s41586-021-03315-7.

Ngou BPM, Ding P, Jones JD. Thirty years of resistance: Zig-zag through the plant immune system. Plant Cell. 2022;34(5):1447–78. https://doi.org/10.1093/plcell/koac041.

Niderman T, Genetet I, Bruyère T, Gees R, Stintzi A, Legrand M, et al. Pathogenesis-related PR-1 proteins are antifungal. Isolation and characterization of three 14-kilodalton proteins of tomato and of a basic PR-1 of tobacco with inhibitory activity against *Phytophthora infestans*. Plant Physiol. 1995;108(1):17–27. https://doi.org/10.1104/pp.108.1.17.

Pruitt RN, Locci F, Wanke F, Zhang L, Saile SC, Joe A, et al. The EDS1–PAD4–ADR1 node mediates Arabidopsis pattern-triggered immunity. Nature. 2021;598(7881):495–9. https://doi.org/10.1038/s41586-021-03829-0.

Sang Y, Macho AP. Analysis of PAMP-triggered ROS burst in plant immunity. In: Shan L, He P, editors. Plant pattern recognition receptors: methods and protocols. New York: Springer; 2017. p. 143–53. https://doi.org/10.1007/978-1-4939-6859-6_11.

Sharma A, Badola PK, Bhatia C, Sharma D, Trivedi PK. Primary transcript of miR858 encodes regulatory peptide and controls flavonoid biosynthesis and development in Arabidopsis. Nat Plants. 2020;6(10):1262–74. https://doi.org/10.1038/s41477-020-00769-x.

Sung YC, Outram MA, Breen S, Wang C, Dagvadorj B, Winterberg B, et al. PR1-mediated defence via C-terminal peptide release is targeted by a fungal pathogen effector. New Phytol. 2021;229(6):3467–80. https://doi.org/10.1111/nph.17128.

Tian H, Wu Z, Chen S, Ao K, Huang W, Yaghmaiean H, et al. Activation of TIR signalling boosts pattern-triggered immunity. Nature. 2021;598(7881):500–3. https://doi.org/10.1038/s41586-021-03987-1.

Tugizimana F, Djami-Tchatchou AT, Steenkamp PA, Piater LA, Dubery IA. Metabolomic analysis of defense-related reprogramming in *Sorghum bicolor* in response to *Colletotrichum sublineolum* infection reveals a functional metabolic web of phenylpropanoid and flavonoid pathways. Front Plant Sci. 2019. https://doi.org/10.3389/fpls.2018.01840.

Ullah C, Unsicker SB, Fellenberg C, Constabel CP, Schmidt A, Gershenzon J, et al. Flavan-3-ols are an effective chemical defense against rust infection. Plant Physiol. 2017;175(4):1560–78. https://doi.org/10.1104/pp.17.00842.

Vitale S, Di Pietro A, Turrà D. Autocrine pheromone signalling regulates community behaviour in the fungal pathogen *Fusarium oxysporum*. Nat Microbiol. 2019;4(9):1443–9. https://doi.org/10.1038/s41564-019-0456-z.

Vlot AC, Klessig DF, Park S-W. Systemic acquired resistance: the elusive signal(s). Curr Opin Plant Biol. 2008;11(4):436–42. https://doi.org/10.1016/j.pbi.2008.05.003.

Wan S, Xin X-F. Regulation and integration of plant jasmonate signaling: a comparative view of monocot and dicot. J Genet Genomics. 2022;49(8):704–14. https://doi.org/10.1016/j.jgg.2022.04.002.

Wen T, Zhao M, Yuan J, Kowalchuk GA, Shen Q. Root exudates mediate plant defense against foliar pathogens by recruiting beneficial microbes. Soil Ecol Lett. 2021;3(1):42–51. https://doi.org/10.1007/s42832-020-0057-z.

Woloshuk CP, Meulenhoff JS, Sela-Buurlage M, Elzen P, Cornelissen B. Pathogen-induced proteins with inhibitory activity toward *Phytophthora infestans*. Plant Cell. 1991;3(6):619–28. https://doi.org/10.1105/tpc.3.6.619.

Yang J, Zhang Y. I-TASSER server: new development for protein structure and function predictions. Nucleic Acids Res. 2015;43(W1):W174–81. https://doi.org/10.1093/nar/gkv342.

Yang Q, Yang J, Wang Y, Du J, Zhang J, Luisi BF, et al. Broad-spectrum chemicals block ROS detoxification to prevent plant fungal invasion. Curr Biol. 2022;32(18):3886–97. https://doi.org/10.1016/j.cub.2022.07.022.

Yin C, Casa Vargas JM, Schlatter DC, Hagerty CH, Hulbert SH, Paulitz TC. Rhizosphere community selection reveals bacteria associated with reduced root disease. Microbiome. 2021;9(1):86. https://doi.org/10.1186/s40168-020-00997-5.

Yuan M, Jiang Z, Bi G, Nomura K, Liu M, Wang Y, et al. Pattern-recognition receptors are required for NLR-mediated plant immunity. Nature. 2021;592(7852):105–9. https://doi.org/10.1038/s41586-021-03316-6.
Zaynab M, Fatima M, Abbas S, Sharif Y, Umair M, Zafar MH, et al. Role of secondary metabolites in plant defense against pathogens. Microb Pathog. 2018;124:198–202. https://doi.org/10.1016/j.micpath.2018.08.034.
Zhang L, Ni H, Du X, Wang S, Ma X-W, Nürnberger T, et al. The *Verticillium*-specific protein VdSCP7 localizes to the plant nucleus and modulates immunity to fungal infections. New Phytol. 2017;215(1):368–81. https://doi.org/10.1111/nph.14537.
Zhang J, Yan H, Xia M, Han X, Xie L, Goodwin PH, et al. Wheat root transcriptional responses against *Gaeumannomyces graminis* var. *tritici*. Phytopathol Res. 2020;2:23. https://doi.org/10.1186/s42483-020-00066-7.
Zhang N, Song L, Xu Y, Pei X, Luisi BF, Liang W. The decrotonylase FoSir5 facilitates mitochondrial metabolic state switching in conidial germination of *Fusarium oxysporum*. Elife. 2021;10:e75583. https://doi.org/10.7554/eLife.75583.
Ziemann S, van der Linde K, Lahrmann U, Acar B, Kaschani F, Colby T, et al. An apoplastic peptide activates salicylic acid signalling in maize. Nat Plants. 2018;4(3):172–80. https://doi.org/10.1038/s41477-018-0116-y.
Zipfel C. Pattern-recognition receptors in plant innate immunity. Curr Opin Immunol. 2008;20(1):10–6. https://doi.org/10.1016/j.coi.2007.11.003.